한국정밀공학회지 제 36 권 제 6 호 pp. 583-590
J. Korean Soc. Precis. Eng., Vol. 36, No. 6, pp. 583-590
June 2019 / 583
https://doi.org/10.7736/KSPE.2019.36.6.583
ISSN 1225-9071 (Print) / 2287-8769 (Online)

Check for updates

운동 방정식을 기초로 한 새로운 단면 밸런싱 기법

A New Single-Plane Balancing Method Based on Equations of Motion

박노길[1,#]
Nogill Park[1,#]

1 부산대학교 기계공학부 (School of Mechanical Engineering, Pusan National University)
Corresponding Author / E-mail: parkng@pnu.edu, TEL: +82-51-510-2325
ORCID: 0000-0002-3922-9975

KEYWORDS: Influence coefficient method (영향계수법), Shaft bow (축 휨), Phase angle measurement (위상각 측정), Heavy spot (질량 쏠림점), High spot (휨 쏠림점), Parameter identification (매개변수 추출)

This study presents a new balancing method that utilizes the equations of motion associated with the rotor dynamics system. While the conventional balancing method includes calculation of mass unbalance based on so-called as-is and trial-run techniques, the proposed approach computes mass unbalance by only applying the as-is technique and further explains the critical speed and the damping ratio. A simple test rig was employed to validate the efficacy of the proposed method. A non-central rotor system was utilized as the experimental model, the actual value of the rotor system's mass eccentricity was measured according to ISO 1940/1-1986(E), and with a comparison done using the results obtained by applying the proposed method. The sensitivity of the measurement error was compared with that of the conventional approach which utilizes the influence coefficient method.

Manuscript received: February 22, 2019 / Accepted: February 25, 2019

NOMENCLATURE

C = Damping
e_b = Magnitude of shaft bow
e_u = Eccentricity of mass unbalance
$\mathbf{F_u}$ = Complex exciting force due to mass unbalance
K = Stiffness
M = Mass
r = Whirl motion of rotor
R = Response of whirl motion
U_u = Magnitude of mass unbalance
ζ = Damping ratio
Ψ_b = The phase angle of the shaft bow from the key phaser
ψ_m = The phase angle of the heavy spot from the key phaser
Ω = Rotational speed
Ω_{cr} = Critical speed

1. Introduction

As machines rotate at progressively higher speeds, vibration becomes a significant problem. There is a need to develop vibration-control techniques for the increasing speeds of modern technology. Balancing techniques are the most accurate and reliable way to eliminate many sources of vibration, and much of the current research focuses on this area. However, the currently used balancing techniques are based on the finite influence coefficient method, which was first introduced in 1934 and few advances have been introduced since that time. The technique is nevertheless popular because it can be deployed without advanced knowledge of rotor dynamics. However, it does not yield accurate results in applications that, due to a low tolerance for measurement errors, require precise balancing. Since Jeffcott[1] introduced the whirl motion equations for a disk on a symmetrical axis, research on rotor dynamics analysis has shown

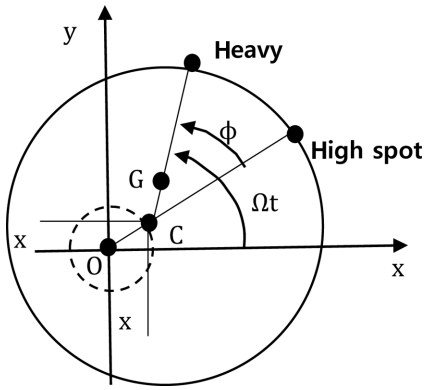

Fig. 1 Mathematical model for rotor dynamic analysis

steady progress and the accuracy of the mathematical models have improved substantially. Despite these developments, advanced analytical and modeling techniques are not being utilized in balancing.

EI-Shafei et al. claim that balancing can be achieved without a trial run by using the calibrated rotor model, which contains data regarding the initial balancing performed during the manufacturing of the rotor.[2] This approach, however, is not completely new because it uses the conventional influence coefficient method for establishing the initial calibrated rotor model. Although modal balancing is an advanced balancing technique that uses a decoupling procedure, it is still an influence coefficient method.

The basic concept of the influence coefficient method is to regard the transfer function of the rotor dynamics system as a coefficient that is obtained through a calibration process according to the trial weight. In this way the amount of unbalance is determined. In this process, however, the physical parameters regarding the mass, damping, and stiffness elements of the rotor dynamics system are not separately incorporated but are instead combined into a single coefficient. Consequently, the equations of motion lose their significance and only the linear relationship between unbalance and whirl motion is used. In other words, the balancing technique is based on a simplified linear relationship rather than on equations of motion. Accordingly, analytical processes, such as mathematical modeling and deriving equations of motion, become unnecessary in balancing. In this study, single-plane balancing is achieved based on equations of motion. For this purpose, the issue of balancing is regarded as a system-identification problem based on an explanation of the amount of unbalance by using measured motion data. Therefore, the basis of the algorithm is derived from the equations of motion obtained from a mathematical model. A non-central disk on a flexible shaft model[3] is used to verify the efficacy of the proposed method. A test rig is designed and implemented, and the true value of the rotor system's mass eccentricity is measured according to ISO 1940/1-1986(E). By using the proposed method, the mass eccentricity, critical speed, and damping ratio of the experimental model is obtained and compared with the true value. The sensitivity of measurement error is compared with the influence coefficient method.

2. Rotor Dynamics Analysis and Rotor Balancing Technique

2.1 Classical Mathematical Model for Rotor Dynamics Analysis

The whirl-motion dynamics of a rotor on an axis was explained by Jeffcott[1] in 1919 and signified a turning point in rotor dynamics. The focal point of Jeffcott's study was the assessment of the trajectory of the rotor's elastic center (in the direction of the line between the spatial center (O) and the elastic center (C) (High Spot)) according to the centrifugal force acting in the direction of the heavy spot, the line between the elastic center (C), and the center of mass (G).

Jeffcott also demonstrated that the dynamic behavior of the high spot, or the unbalanced exciting force, under a normal state is a harmonious motion. A point to note is that the phase angle of the heavy spot is defined from the horizontal line (OX) of the fixed space. It causes that the phase angle of the heavy spot from the key phaser as a system parameter is not expressed in the derived equation of motion. The equations of motion are derived in Jeffcott's paper as follows:

$$M\ddot{\mathbf{r}}+C\dot{\mathbf{r}}+K\mathbf{r}=U_u\Omega^2e^{j\Omega t} \tag{1}$$

$$U_u=Me_u \tag{2}$$

Where $\mathbf{r}(=x+yj)$ is whirl motion of the elastic center. The phase angle of the high spot ($\angle$xOC) was obtained as the relative position angle ϕ of the heavy spot as follows:

$$\phi=\tan^{-1}\left(\frac{C\Omega}{K-M\Omega^2}\right) \tag{3}$$

Although Jeffcott did not define the heavy spot's phase angle as the reference of the key phaser and did not indicate clearly the phase angle of the heavy spot, he defined the relative position angle ϕ, thereby making his analysis complete and not debatable.

But the derived Eq. (1) is not able to use for the balancing technique because of neglecting the the phase angle of the heavy spot from the key phaser.

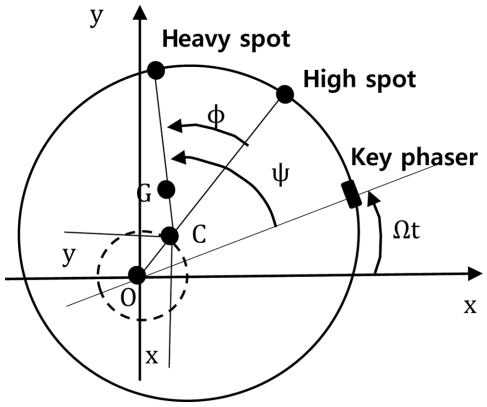

Fig. 2 Mathematical model for rotor balancing technique

2.2 Mathematical Model for Rotor Balancing Technique

The influence coefficient method was first introduced by Thearle in 1934 and has been widely used in academic and industrial applications, and is now considered to be the classic balancing technique. In 1992, Ehrich described the influence coefficient method by first introducing the Jeffcott rotor's equations of motion.[4] Although Ehrich's equations of motion are almost identical to the ones derived by Jeffcott, Ehrich's equations are more advanced because the heavy spot is expressed by using complete equations. As shown in Fig. 2, Ehrich defined the phase angle of the heavy spot by using the fixed-space reference line (x Axis) and the rotor reference line (Key Phaser). The whirl motion (**r**) and the exciting force ($\mathbf{F_u}$) due to mass unbalance were expressed in complex numbers. The phase angle ψ signified the phase angle of the heavy spot with reference to the key phaser in Fig. 2. And Ωt was the phase angle of the key phaser varying in time with reference to the horizontal line. Therefore, $\mathbf{F_u}$ was completely defined as follows:

$$\mathbf{F_u} = M\mathbf{e_u}\Omega^2 e^{j\Omega t} \tag{4}$$

$$\mathbf{e_u} = e_u e^{j\psi} \tag{5}$$

Therefore the equation of motion of the unbalance exciting force is written as follows:

$$M\ddot{\mathbf{r}} + C\dot{\mathbf{r}} + K\mathbf{r} = \mathbf{F_u} = Me_u\Omega^2 e^{j\Omega t} \tag{6}$$

Where **r** is a position vector from O to C and $\mathbf{e_u}$ is a position vector from C to G. Assuming synchronous motion, we have

$$\mathbf{r} = \mathbf{R}e^{j\Omega t} \tag{7}$$

And by transforming Eq. (6) into the frequency domain, the steady state response of whirl motiom **R** is derived as follows:

$$\mathbf{R} = \mathbf{A}(\Omega)M\mathbf{e_u} \tag{8}$$

$$\mathbf{A}(\Omega) = \frac{\Omega^2}{K - M\Omega^2 + j\Omega C} \tag{9}$$

Where **A**(Ω) is the mechanical impedance of Jeffcott rotor. Eq. (8) represents that the complex response of whirl motion is proportional to the complex mass-unbalance during constant speed, which is basic concept of influence coefficient method. Eq. (9) is referred to as the influence coefficient, and it expresses the relationships among the parameters associated with the mass, damping, and stiffness elements of the rotor dynamics system. However, the influence coefficient method does not use the relationship in Eq. (9) but simply processes the mechanical impedance **A**(Ω) as a complex coefficient while fixing the operation speed.

In Eq. (8), **R** is a measured value, and the amount of unbalance $M\mathbf{e_u}$ and the influence coefficient **A**(Ω) are unknown. Since the two unknown values cannot be obtained from Eq. (8) alone, a trial run is performed. By adding a trial mass ($\mathbf{U_t}$), **R**′ is measured again at an identical operation speed to obtain another equation:

$$\mathbf{R}' = \mathbf{A}(\Omega)(M\mathbf{e_u} + \mathbf{U_t}) \tag{10}$$

Therefore, the influence coefficient **A**(Ω) and the mass unbalance $M\mathbf{e_u}$ can now be obtained from Eqs. (8) and (10). Consequently, the highlight of the influence coefficient method is to identify the magnitude and phase angle of complex eccentricity $\mathbf{e_u}$ by adding trial-mass process. Here the merit of the influence coefficient method is that the mechanical impedance **A**(Ω) can be treated as a constant value. As a result, the mathematical modeling processes are not necessary any more. In some practical aspect, it would be true. But in precision engineering aspect, it might be stupid to use no more the works established in the rotor dynamic analysis field.

This implies that the approach is very useful in field applications because balancing can be achieved by non-experts without an understanding of the mathematical modeling of the rotor dynamics system. On the other hand, it is also true that the advanced rotor dynamics modeling techniques that have been introduced since 1919 cannot be applied to the balancing technique. We believe that balancing can be viewed as an inverse problem, where the whirl motion is measured and the mass unbalance that caused the whirl can be explained. If so, there should be an interaction between the balancing technique and the techniques of analyzing rotor dynamics systems, but the two areas remain very much independent. In order to help establish an essential relationship between these two areas, we propose a new balancing technique that incorporates both Eqs. (8) and (9).

3. A New Balancing Technique Based on Equations of Motion

3.1 Jeffcott Rotor with Shaft Bow

This paper proposes a new balancing technique based on equations of motion. As a sample system, a schematic of a Jeffcott rotor with shaft bow is considered in Fig. 3. For the generality of measurement, a gap sensor that measures the high spot is placed at a phase angle λ on the opposite side of the x axis. A photo sensor that indicates the position of the key phaser is placed along the +x axis. For the elastic center, the equation of motion at the center of mass G is derived as follows:

$$M\ddot{\mathbf{r}}+C\dot{\mathbf{r}}+K(\mathbf{r}-\mathbf{e_b})=\mathbf{F_u} \tag{11}$$

where $\mathbf{e_b}$ is the position vector from O to B expressed in complex numbers. This value may be either known or unknown according to the situation of the rotor system. The third term of Eq. (11) $K(\mathbf{r}-\mathbf{e_b})$ is the restoring force reacting at the elastic center C due to the elastic deformation of the rotor shaft. For the simplicity, in this paper, $\mathbf{e_b}$ is assumed to be prescribed one. And the nonhomogeneous term of Eq. (11) $\mathbf{F_u}e^{j\Omega t}$ represents the centrifugal force by the eccentricity applying out from C to G. The magnitude of the centrifugal force is $Me_u\Omega^2$ and the phase angle of $\mathbf{F_u}$ is the cosine angle between line $\overline{CG}$ and x-axis, $\Omega t+\psi_m$ shown in in Fig. 3. Therefore we have,

$$\mathbf{F_u}=(Me_u\Omega^2)e^{j(\Omega t+\psi_m)}=M\mathbf{e_u}\Omega^2e^{j\Omega t} \tag{12}$$

$$\mathbf{e_u}=e_ue^{j\psi_m} \tag{13}$$

Similarly, in Fig. 3, we have

$$\mathbf{e_b}=e_be^{j(\Omega t+\psi_b)}=(e_be^{j\psi_b})e^{j\Omega t} \tag{14}$$

Where e_b and ψ_b can be measured while slow speed. Therefore substituting Eqs. (12)-(14) into Eq. (11), we obtain the final form of equation of motion about the Jeffcott rotor with shaft bow as follows:

$$M\ddot{\mathbf{r}}+C\dot{\mathbf{r}}+K\mathbf{r}=(M\mathbf{e_u}\Omega^2)e^{j\Omega t}+(K\mathbf{e_b})e^{j\Omega t}$$

Dividing by mass M, finally, we have

$$\ddot{\mathbf{r}},2\zeta\Omega_{cr}\dot{\mathbf{r}}+\Omega_{cr}{}^2\mathbf{r}=(\Omega^2\mathbf{e_u}+\Omega_{cr}{}^2\mathbf{e_b})e^{j\Omega t} \tag{15}$$

Where $2\zeta\Omega_{cr}$ and $\Omega_{cr}{}^2$ are unknown natural characteristic parameters of Jeffcott rotor. And also, substituting Eq. (7) into

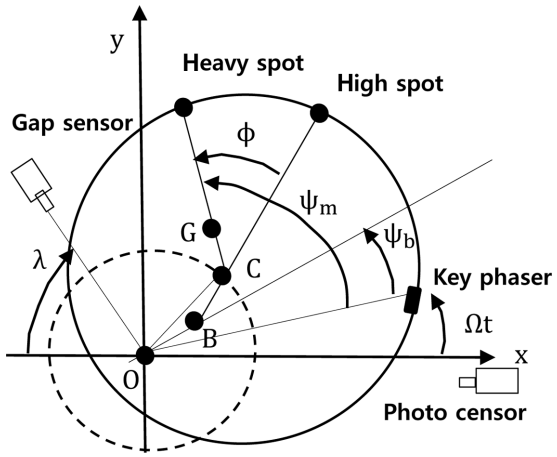

Fig. 3 Whirl motion of Jeffcott rotor with shaft bow

Eq. (15), we have,

$$\{(\Omega_{cr}{}^2-\Omega^2)+j(2\zeta\Omega_{cr})\}\mathbf{R}=\Omega^2\mathbf{e_u}+\Omega_{cr}{}^2\mathbf{e_b} \tag{16}$$

Based on Eq. (16), we can identify the natural characteristic parameters $2\zeta\Omega_{cr}$ and $\Omega_{cr}{}^2$ as well as the target unknown eccentricity $\mathbf{e_u}$. Then Eq. (16) contains four unknowns and two equations. To obtain these unknown values, more than two operational speeds. Let them be Ω_1 and Ω_2. Then applying them into Eq. (16), we have

$$\{(\Omega_{cr}{}^2-\Omega_1{}^2)+j(2\zeta\Omega_{cr})\}\mathbf{R}_1=\Omega_1{}^2\mathbf{e_u}+\Omega_{cr}{}^2\mathbf{e_b} \tag{16}$$

$$\{(\Omega_{cr}{}^2-\Omega_2{}^2)+j(2\zeta\Omega_{cr})\}\mathbf{R}_2=\Omega_2{}^2\mathbf{e_u}+\Omega_{cr}{}^2\mathbf{e_b} \tag{17}$$

Solving (16) and (17), we obtain the unknowns, $\Omega_{cr}{}^2$, $2\zeta\Omega_{cr}$, e_u, and ψ_m without trial mass process.

Compensation mass unbalance $\mathbf{U_c}(=m\mathbf{e_c})$ is obtained as following relationship:

$$\mathbf{U_c}\Omega^2+M\mathbf{e_u}\Omega^2+K\mathbf{e_b}=0$$

So, we have

$$\mathbf{U_c}=-\left\{M\mathbf{e_u}+\frac{K}{\Omega^2}\mathbf{e_b}\right\}=-M\left\{\mathbf{e_u}+\left(\frac{\Omega_{cr}}{\Omega}\right)^2\mathbf{e_b}\right\} \tag{18}$$

4. Verification Experiment

4.1 Test Rig

A simple test rig was implemented to verify the efficacy of the new balancing technique proposed in this study. As shown in Fig. 4, the rotor cylinder was placed on a steel axis and was supported

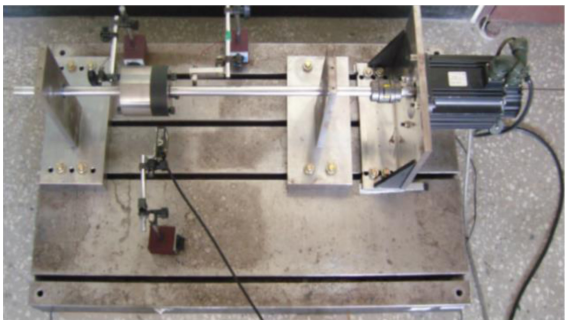

Fig. 4 Test rig

by ball bearings across a 580 mm span. The rotor was positioned to the left of the center of the bearing support. The axis was connected directly to the driving motor and the two were linked by using a coupling. The ratio of the cylinder length to its diameter was 1.0, and the critical speeds in the cylindrical and conical modes were 3500 and 73000 rpm, respectively. Twelve holes were drilled at the 40-mm position on the radius to attach trial weights to both sides of the rotor, with each hole capable of holding up to 24 g of trial weight (Fig. 5). The rotation axis was sustained with ball bearings (No. 6004) at both ends, and the length of the support unit was 580 mm. The rotation axis was connected to a 3000-W inductor motor via a rubber coupling. There was some backlash through the coupling between the motor and the rotation axis. Also, there was misalignment in the permanent shaft bow, rotation axis, and motor axis. As shown in Fig. 3, the photo sensor and two gap sensor were installed horizontally ($\lambda = 0°$). Two gap sensors were placed in identical locations on both sides to measure the whirl motion, as displayed in Fig. 4. One photo sensor was prepared to trace the position of the key phaser. The whirl motion necessary for single-plane balancing was obtained by calculating the average of the whirl motions as measured by the two gap sensors. The new single-plane balancing technique proposed in this paper involves the following procedure:

Step 1. Measurement of whirl motion at slow speed 400 rpm without a trial weight to measure the shaft bow: $\mathbf{e_b}$.

Step 2. Measurement of whirl responses $\mathbf{R_1}$ (Ω_1 is chosen at around 1500 rpm) and $\mathbf{R_1}$ (Ω_2 is chosen at around 2100 rpm)

Step 3. Calculation of Ω_{cr}^2, $2\zeta\Omega_{cr}$, e_u, and ψ_m from Eqs. (16) and (17).

Step 4. Caculation of compensation mass unbalance $\mathbf{U_c}$ from Eq. (18) to perform balancing.

4.2 Measurement of Whirl Response R

The complex whirl response **R** is measured by a photo sensor and a gap sensor. The measured time-domain signal **r** of Eq. (7)

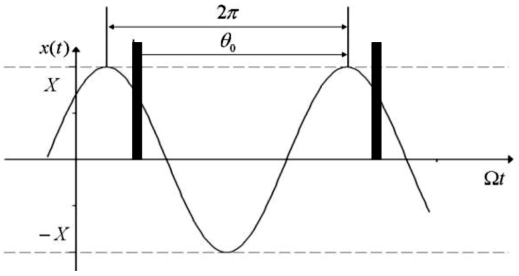

Fig. 5 The relationship between the phase angle and the wave form on oscilloscope

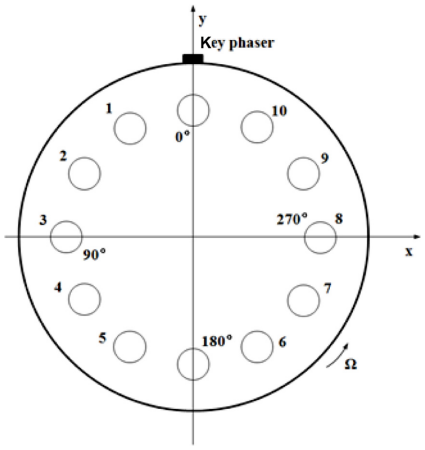

Fig. 6 Installation angles of the added masses

is displayed on the on oscilloscope. The sinusoidal curve shown in Fig. 5 depicts the time domain signal picked up by the gap sensor. And the pulse signal is picked up by a photo sensor. We can read a pick-to-pick value and the phase angle θ_0.

From Fig. 5, the amplitude R is the half of pick-to-pick value 2X and the phase angle of complex value **R** becomes $2\pi - \theta_0 - \lambda$. That is, we have

$$\mathbf{R} = Xe^{j(2\pi-\theta_0-\lambda)} = Xe^{-j(\theta_0+\lambda)} \tag{19}$$

4.3 Measurement of the True Value of Mass Unbalance

We must know the true value of the mass unbalance for the experimental model in advance in order to verify the efficacy of the proposed technique. The true value was obtained based on experiment according to Section 8 “Determination of the residual unbalance” in ISO 1940/1-1986(E). As shown in Fig. 6, after the trial weights are placed into the rotor holes at equal intervals, unbalance is obtained by using the influence coefficient method, and the average unbalance is regarded as the true value.

The main vibration sources of the experimental model are rotor unbalance, shaft bow, and misalignment between the motor and the axis. The run-out caused by shaft bow and misalignment were measured by using the convergent value as the speed was

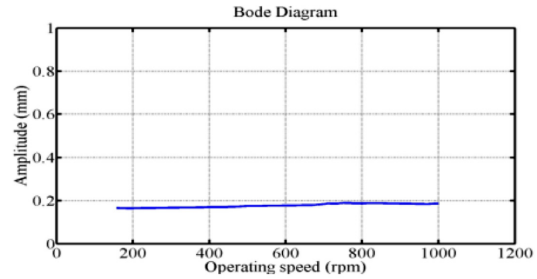

(a) $|\mathbf{e_b}|$

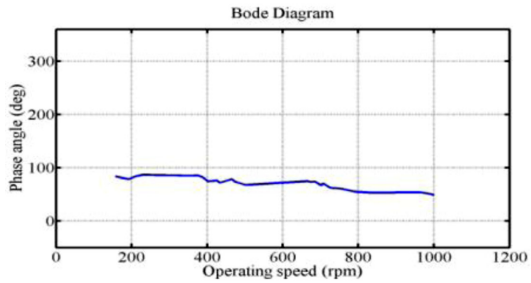

(b) $\angle\mathbf{e_b}$

Fig. 7 Measured run-out

decreased from 1000 rpm. As indicated in Fig. 7, there was no variation in the whirl motion below 400 rpm. The experimental results indicate that run-out occurred at 0.17(mm)∠75°, which was regarded as $\mathbf{e_b}$ in Eq. (14): $\mathbf{e_b} = 0.17e^{j\left(\frac{75\pi}{180}\right)} = 0.164 + 0.044j$.

The true value of the mass unbalance of the experimental model $\overline{\mathbf{e_u}}$ was obtained according to ISO 1940/1-1986(E). The whirl motions without run-out are measured at sampling speeds of 1500 and 2100 rpm, and the results are depicted on a complex plane in Fig. 8. The average of these values was 0.23(mm) ∠294°, which was the true value of the experimental model: $\mathbf{e_u} = 0.23e^{j\left(\frac{294\pi}{180}\right)} = 0.094 - 0.210j$.

4.4 Single-Plane Balancing Based on the Proposed Method

This section explains the mass eccentricity of the experimental model $\mathbf{e_u}$ according to the proposed method. Whirl responses $\mathbf{R_1}$ and $\mathbf{R_2}$ were measured at 1500-2600 rpm. Sampling is carried out with two categories; low speed range (1500-2000 rpm) for $\mathbf{R_1}$ and high speed range (2000-2600 rpm) for $\mathbf{R_2}$. Table 1 lists the magnitudes and phase angles of the whirl responses. Two of the whirl responses were selected in Tabls 1(a) and 1(b), respectively and used in Eqs. (1) and (17).

The identified $\mathbf{e_u}$ by proposed method was chose as the average value, 0.27(mm)∠314° in Table 2. Compared with $\overline{\mathbf{e_u}}$ = 23(mm)∠294° measured according to ISO specifications, The percent errors resulting in magnitude and phase discrepancies are 20% and 2%, respectively. Although there was some discrepancy in magnitude, the phase angle coincided

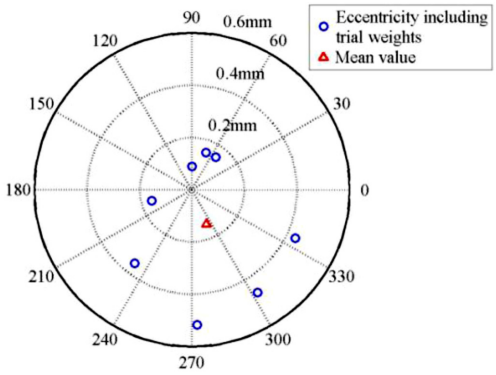

(a) $\overline{\mathbf{e_u}}$ at 1500rpm

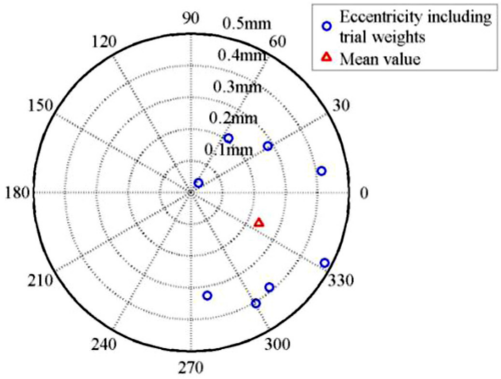

(b) $\overline{\mathbf{e_u}}$ at 2100rpm

Fig. 8 Measuring process of the true value of eccentricity by using the ISO standard

Table 1 Measured whirl response

(a) For $\mathbf{R_1}$

Ω_1 (rpm)	$\lvert\mathbf{R_1}\rvert$ (mm)	$\angle\mathbf{R_1}$ (°)
1538.5	0.18636	∠138.5
1666.7	0.20564	∠140.0
1764.7	0.21862	∠142.9
1818.2	0.22961	∠147.3
1935.5	0.24101	∠156.8

(b) For $\mathbf{R_2}$

Ω_2 (rpm)	$\lvert\mathbf{R_2}\rvert$ (mm)	$\angle\mathbf{R_2}$ (°)
2222.2	0.29987	∠173.3
2307.7	0.33809	∠180.0
2400.0	0.36280	∠180.0
2500.0	0.42914	∠195.0
2608.7	0.46103	∠211.3

excellently. In addition to mass eccentricity, the proposed method provides critical speed and damping ratios of 3113 rpm and 0.012, respectively.

The compensation weight was calculated from Eq. (18) based on the mass eccentricities obtained in this section, and balancing

Table 2 Parameter identifications by proposed balancing technique

Sampling speeds(rpm)		Identified parameters (mm, °, rpm)			
Ω_1	Ω_2	e_u	ψ_m	Ω_{cr}	ζ
1538.	2222.	0.4209	∠315.8	3438.	0.0059
	2307.	0.3779	∠313.6	3298.	0.0068
	2400.	0.4687	∠317.7	3585	0.0050
	2500.	0.3402	∠312.5	3232.	0.0097
	2608.	0.2876	∠310.4	3135.	0.0139
1666.	2307.	0.2212	∠309.9	2952.	0.0121
	2400.	0.2720	∠317.2	3192.	0.0115
	2500.	0.2720	∠312.0	3011.	0.0124
	2608.	0.2048	∠310.2	2962.	0.0146
1764.	2400.	0.2275	∠316.7	3094.	0.0131
	2500.	0.2012	∠311.3	2950.	0.0130
	2608.	0.1823	∠309.9	2912.	0.0148
1818.	2500.	0.2095	∠316.0	2989.	0.0145
	2608.	0.1854	∠314.3	2929.	0.0162
1935.	2608.	0.2208	∠315.8	3009.	0.0166
Average		0.2697	∠313.9	3113.	0.012

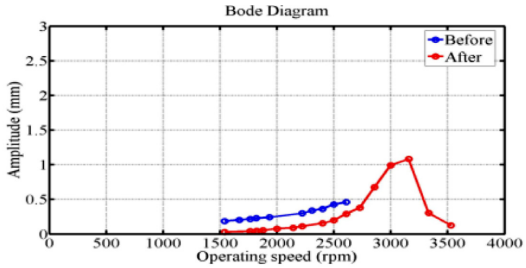

(a) Amplitude |**R**|

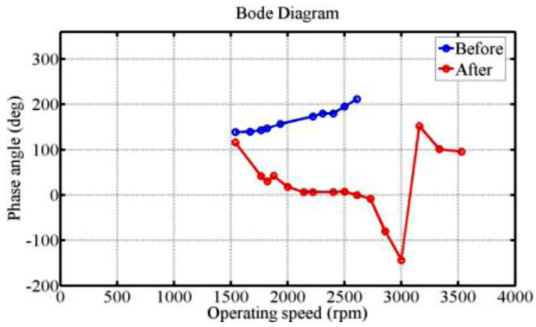

(b) Phase ∠**R**

Fig. 9 Bode plot of the whirl response

was performed and passed the first critical speed. Fig. 9 displays the whirl response before and after balancing. According to observation, the critical speed was 3157 rpm and the damping ratio was approximately 0.052. After balancing, there was a 1.4%

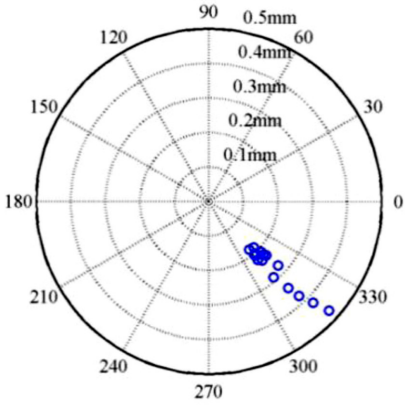

(a) Proposed Method

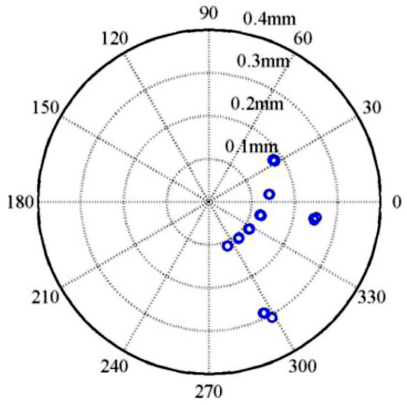

(b) Influence Coefficient Method

Fig. 10 Deviations in unbalance

error in critical speed and damping improved by 77%. The experimental results indicate that the proposed method yielded a result close to the true value and the critical speed was predicted with a high level of accuracy.

4.5 Effect on Measurement Error

The balancing technique is sensitive toward measurement error. In order to assess the effect of the proposed method on measurement error, the experimental parameters used in the measurement were applied to the influence coefficient method to compare with the results obtained by using the proposed method. The influence coefficient method requires as-is and trial-run measurements. Two measurements at 1538.5 and 2222.2 rpm used in single-plane balancing were set as as-is values, and three separate experiments were conducted at 1500 and 2100 rpm, and their average was used as the trial-run value to obtain mass eccentricity. Fig. 10 displays the mass eccentricity distributions displayed by the proposed method and the influence coefficient method. As the figure indicates, the proposed method converges more accurately to the phase of mass eccentricity than does the influence coefficient method.

5. Conclusion

A new balancing technique employing equations of motion was proposed and its efficacy was experimentally verified to obtain the following conclusions:

(1) The magnitude and the phase of the mass eccentricity obtained by using the proposed method displayed errors of 20% and 2%, respectively, from ISO specifications.

(2) The critical speed and the damping ratio obtained by using the proposed method were consistent excellently with the experimental results.

(3) The proposed method is less sensitive toward measurement error than the influence coefficient method.

(4) By one shot run, the single balancing is successively carried out without a trial mass process.

The proposed method can be conceptually applied to the multiple balancing technique.

ACKNOWLEDGEMENT

This work was supported by a 2-Year Research Grant of Pusan National University.

REFERENCES

1. Jeffcott, H. H., “The Lateral Vibration of Loaded Shafts in the Neighbourhood of a Whirling Speed–The Effect of Balance,” The London, Edinburgh and Dublin Philosophical Magazine and Journal of Science, Vol. 37, No. 219, pp. 304-314, 1919.
2. EI-Shafei, A., EI-Kabbany, A. S., and Younan, A. A., “Rotor Balancing Without Trial Weights,” Journal of Engineering for Gas Turbines and Power, Vol. 126, No. 3, pp. 604-609, 2004.
3. Krämer, E., “Dynamics of Rotors and Foundations,” Springer Verlag,” pp. 1-383, 1993.
4. Ehrich, F. F, “Handbook of Rotordynamics,” McGraw-Hill, pp. 1-496, 1992.

Nogill Park
Ph.D. candidate in the Division of Mechanical Engineering, Pusan National His/Her research interest is Gear Synthesis Analysis.
E-mail: parkng@pnu.edu